

The August 16, 2012 earthquake near Huizinge (Groningen)

Bernard Dost and Dirk Kraaijpoel

KNMI, De Bilt January 2013

Samenvatting

In dit rapport worden de resultaten gepresenteerd van onderzoek door het KNMI naar de aardbeving van 16 augustus 2012 bij Huizinge, gemeente Loppersum, in de provincie Groningen. De locatie van de aardbeving is berekend met behulp van een lokaal snelheidsmodel van de ondergrond en lokale acceleratie data. Resultaat is een verplaatsing van ca 0.5 km naar het westen ten opzicht van de eerste analyse. De sterkte van de beving is geanalyseerd door de moment magnitude te berekenen. Deze komt uit op $M_w = 3.6$ met een onzekerheid van 0.1 magnitude units. De berekende lokale magnitude is 3.4 ± 0.1 . De relatie tussen M_L en M_w wordt nader onderzocht en kan leiden tot een bijstelling van de procedures voor de bepaling van de M_L . In de verdere analyse wordt uitgegaan van een magnitude 3.6 voor dit event.

Berekeningen geven aan dat de bron een gemiddelde beweging van 5 ± 3 cm omvatte langs een cirkelvormig breukoppervlak met een straal van 390 ± 110 m en een spanningsval van 25 ± 9 bar. Deze bepalingen gaan uit van het Brune model. Het mechanisme van de breuk is niet eenduidig te bepalen uit de polariteit van de geregistreerde golven. Onderzoek met behulp van golfvorminversie zal naar verwachting meer duidelijkheid geven. Meerdere S-golven zijn bij deze beving geregistreerd, hetgeen de duur van de sterk gevoelde beweging verlengd heeft. Dit is ook gemeld door de lokale bevolking.

Data van het accelerometer netwerk in het Groningen veld heeft maximale versnellingen (PGA) gemeten tot een maximum van 85 cm/s^2 , of daarvan afgeleid 3.45 cm/s als maximale snelheid (PGV). Vergelijking met voor geïnduceerde bevingen afgeleide relaties tussen de kans op schade en de snelheid van de bodembeweging laat zien dat bij deze waarden een kans van 20-35% op schade bestaat. De gemeten PGA en PGV worden goed voorspeld door bestaande Ground Motion Prediction Equations (GMPE's) die afgeleid zijn voor zwakke en ondiepe aardbevingen. Maximum intensiteit VI is berekend voor een beperkt gebied (< 4 km) rond het macroseismisch epicentrum, dat ca 2 km NE van het instrumentele epicentrum is gelegen.

De toename van het aantal bevingen in het Groningen veld (190 events met een $M_L \geq 1.5$) maakt een update van de hazard berekeningen mogelijk. Gebaseerd op een breuk in de trend van de cumulatieve energie rond 2003, wordt de dataset opgedeeld in twee tijdsintervallen: 1991-2003 en 2003-2012. Analyse laat zien dat de frequentie-magnitude relatie in beide segmenten bepaald wordt door dezelfde Gutenberg-Richter (GR) b-waarde, maar een verschillende waarde voor de jaarlijkse hoeveelheid aardbevingen, de GR a-waarde. De hoeveelheid bevingen neemt toe en dit verschijnsel lijkt te correleren met de toegenomen productie.

Het is niet mogelijk gebleken de maximaal mogelijke magnitude voor aardbevingen in het Groningen veld te schatten op basis van de statistiek. Dit wordt veroorzaakt door de specifieke vorm van de frequentie-magnitude relatie voor het veld en is mogelijk beïnvloed door de niet stationariteit van het proces. Verdere studies, waarbij geologische data en geomechanische modellen gebruikt worden, kunnen mogelijk extra informatie geven.

Tenslotte is een vergelijking gemaakt met gas- en olievelden buiten Nederland en de daarin opgetreden geïnduceerde events. Maximale sterktes van bevingen, zoals in de literatuur vermeld, variëren van $M = 4.2$ tot 4.8 . Hieruit wordt de conclusie getrokken dat niet verwacht wordt dat de maximaal mogelijke magnitude groter dan 5 zal worden. Maximale intensiteiten die behoren bij een ondiepe aardbeving met magnitude 4-5, zullen waarschijnlijk in de VI-VII range liggen.

Summary

This report presents the results of the analysis of the August 16, 2012 earthquake near Huizinge in the province of Groningen. The location of the event is refined by using a local velocity model and using additional data from the local acceleration network. The new location is shifted ca 500 m west of the original location. A moment magnitude was calculated and determined at $M_w=3.6 \pm 0.1$, higher than the originally determined local magnitude of $M_L= 3.4 \pm 0.1$. The relation between M_L and M_w is being investigated and a possible recalibration of the local magnitude may be the result. In the further analysis a magnitude 3.6 is used for this event.

The source radius is estimated to be $390 \text{ m} \pm 110\text{m}$, the stress-drop $25 \text{ bar} \pm 9 \text{ bar}$ and the average displacement $5 \text{ cm} \pm 3 \text{ cm}$, all based on the assumption of a Brune model. No stable solution could be found for the mechanism of the event based on polarity data. Further research using waveform modeling techniques is expected to provide results. Multiple S-wave phases have been recorded, extending the duration of the strongest movement. This is in line with reports from the local people.

The regional accelerometer network recorded peak ground acceleration (PGA) values up to 85 cm/s^2 , corresponding to a maximum peak ground velocity (PGV) of 3.45 cm/s . Comparison with damage probability curves for masonry structures, designed for induced seismicity, show a 20-35% probability of damage at these values. Recorded PGA and PGV values are well predicted by existing Ground Motion Prediction Equations, derived for small and shallow earthquakes. Maximum intensity of VI was detected in a limited region ($< 4\text{km}$) around the macroseismic epicenter, located ca 2 km NE of the instrumental epicenter.

The extended dataset for the Groningen field (190 events of $M \geq 1.5$) allows an update of the hazard analysis. Based on cumulative energy trends, the dataset for Groningen was divided into two segments (1991-2003) and (2003-2012). Analysis shows that the frequency-magnitude relations are characterized by a similar value of the Gutenberg-Richter (GR) b-value, but do have a different seismicity rate. Seismicity rate increases with time and seems to coincide with increased production.

The maximum probable magnitude, estimated only for all fields combined in the past, could not be estimated on the basis of the statistics alone for the Groningen field, due to the nature of the frequency-magnitude relation. Further study using geological information and geomechanical modeling may provide additional information.

Based on a comparison with seismicity in hydrocarbon fields outside the Netherlands, where induced events were recorded up to a maximum of $4.2 < M < 4.8$, we conclude that it is not expected that the maximum probable magnitude will exceed a magnitude 5. Intensities associated with a magnitude 4-5 event are expected to be in the VI-VII range.

Contents

Samenvatting	2
Summary	3
Introduction	5
Data	5
Location	6
Magnitude	8
Source mechanism and parameters	10
Peak ground acceleration (PGA) and peak ground velocity (PGV)	13
Damage and PGV	15
Source duration	16
Intensity	17
Implication for hazard analysis	19
Cumulative energy	19
Frequency-magnitude relation	20
Maximum magnitude	21
Conclusions	24
References	25

Introduction

On August 16, 2012 an induced earthquake occurred in the north of the Netherlands near the village of Huizinge in the municipality of Loppersum. We consider the event being induced due to gas exploration from the Groningen field. The magnitude of the event was $M_L=3.4$, calculated using data from the KNMI regional borehole network [1]. The strength of the earthquake is within its uncertainty comparable to the largest event in the region until present, but its effects at the surface were felt more strongly by the population. More than 2000 damage reports have been received by the company responsible for the gas production (NAM).

In this document we present first results of a detailed analysis of the Huizinge event and discuss its impact with respect to the hazard analysis.

Data

The Huizinge event was recorded by the regional KNMI borehole network, the regional accelerometer network and all additional seismic stations in the south of the Netherlands. European seismic stations reported the event at epicentral distances up to 800 km.

Digital seismological data is in general freely available from global and regional networks and organizations are able to build their own virtual networks. The Orfeus Data Center, hosted at the KNMI, plays a key coordinating role in facilitating this European open data exchange.

Data from the KNMI borehole network is available in real-time and feeds into automated location systems (Seiscomp). These systems are in development and the quality of automated locations are being assessed. Data from the accelerometer network are currently only available off-line. Recently a project started to update and expand the accelerometer network in the region and integrate the datastream into the real-time system.

Location

The event was rapidly identified by both the KNMI and major European data centers. However, rapid automatic locations were made publicly available by these centers using openly available real-time data. Notably these are the Geofon data center (<http://geofon.gfz-potsdam.de/>) and the European Mediterranean Seismological Center (EMSC) (<http://www.emsc-csem.org>). Initial automatic locations and magnitude estimates have been later corrected by human interference. Those manual locations are shown in Figure 2.

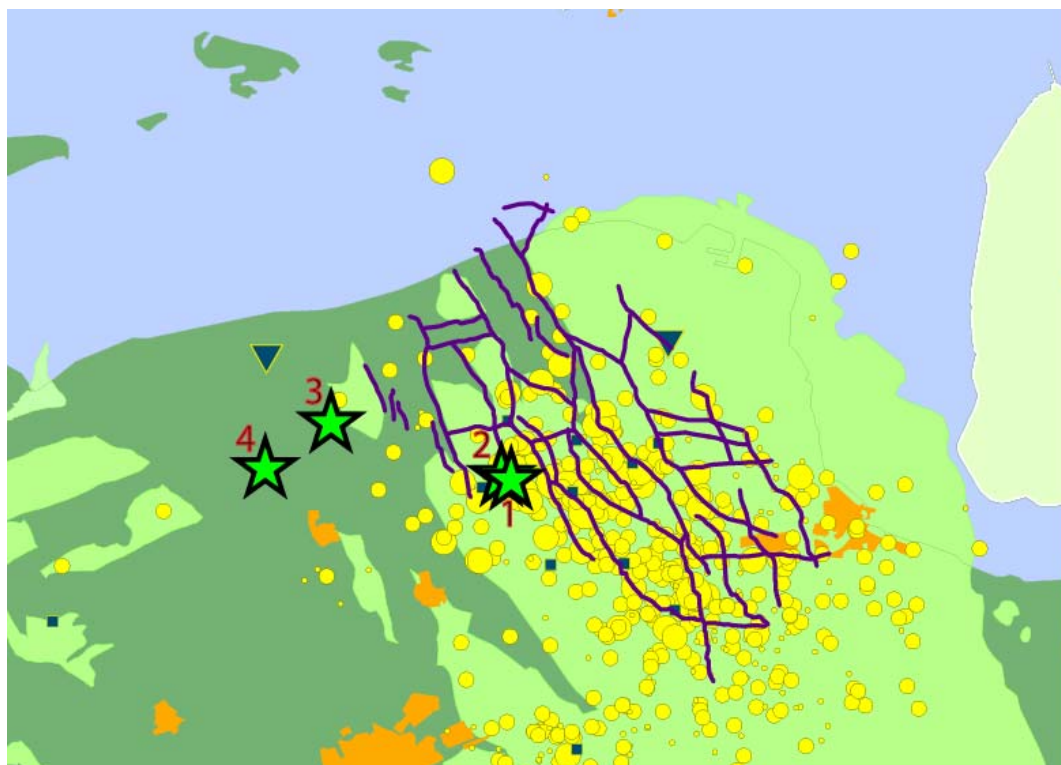


Figure 2. Location of the Huizinge earthquake. The KNMI locations (1- regional model; 2- local model), Geofon location (3) and the EMSC location (4). Gas field are shown in light green, earthquakes as yellow circles, borehole stations by blue inverted triangles and accelerometers by blue squares. Faults at top of the reservoir are indicated by solid lines (data courtesy of NAM).

KNMI location:

Using a regional velocity model and data from the regional borehole network, the KNMI calculated the epicenter at: 53.353 N 6.665 E (in the national coordinate system: X: 240.017 and Y: 596.911). In the source inversion depth has been fixed at 3 km, which is the average depth of the gas fields in the region. Unfortunately, borehole station ENM, located to the North-west was not functioning at the time of the event.

An improved epicenter location was obtained using a local model and including acceleration data from a network of 8 stations that are located within an epicenter distance of 2-10 km. This local model includes a high velocity (salt) layer and does not include a fixed V_p/V_s ratio, but applies the Castagna [14] relation to connect V_p to V_s velocity [2].

Magnitude

For all induced events in the region, the determination of the local magnitude (M_L) at the KNMI is part of the standard processing. For larger events in the Groningen field ($M_L > 2.5$) also moment magnitudes (M_w) have been determined. Within their error bounds both solutions (M_L and M_w) are similar [1]. Evaluation and comparison of both types of magnitudes for the Huizinge event provides us with unique data to possibly recalibrate the local magnitude, a robust, simple and fast magnitude estimate, in relation to the more elaborate but generally more accurate, moment magnitude.

Local magnitude (M_L)

In the standard KNMI analysis the local magnitude is determined, using the KNMI borehole network stations. The local magnitude is defined as $M_L = \log A_{wa} - \log A_0$, where A_{wa} is the maximum amplitude in mm recorded on a simulated Wood-Anderson seismograph and $\log A_0$ is the attenuation function. For the north of the Netherlands an attenuation relation was derived from measurements at borehole sensors at 200m depth [3]:

$$M_L = \log A_{wa} + 1.33 \log(r) + 0.00139r + 0.424$$

where r is the hypocenter distance in km. For each station A_{wa} is measured as the average of the two horizontal components. An average of the 8 most reliable borehole data at a hypocenter distance < 50 km gave a value for the Huizinge event of $M_L = 3.4 \pm 0.1$.

Moment magnitude (M_w)

The moment magnitude is defined as $M_w = (\log(M_0) - 9.1) / 1.5$ [5], where seismic moment M_0 is estimated from the displacement spectra of the data. For a vertically heterogeneous model [6]:

$$M_0 = \frac{4\pi\rho_0^{1/2}\rho_z^{1/2}V_0^{1/2}V_z^{5/2}R}{F_s R_{\theta,\phi}} \Omega_0$$

where ρ is the density, V is the P- or S-wave velocity and the subscripts 0 and z indicate the values at the receiver and at source depth respectively. R is the hypocenter distance, F_s accounts for the free-surface amplification ($F_s=2$) and $R_{\theta,\phi}$ is the average radiation pattern coefficient (0.52 for P-waves and 0.63 for S-waves) and Ω_0 is the low frequency spectral level. Kraaijpoel and Dost [2] determined source parameters for 4 earlier events in the Groningen field and showed a good correspondence between M_L and M_w , using a shear velocity $V_0 = 700$ m/s and a $V_z = 2200$ m/s at a source depth of 3 km. Densities are $\rho_0 = 1960$ kg m⁻³ and $\rho_z = 2600$ kg m⁻³.

The raw data files are corrected for instrument response and absorption/scattering. The latter correction is of the form $e^{\pi f (\frac{R}{Q\beta} + \kappa)}$, with R hypocenter distance, Q the quality factor describing regional anelastic attenuation, β the shear velocity, and κ a measure of the high frequency decay slope [7]. Q was calculated for previous events in the Groningen field and ranges from $Q=20$ for distances < 25 km to 60 at a distance >50 km. The measured values for κ in this region are between 0.02 and 0.05.

After correction for the high frequency attenuation, the S-wave displacement spectra were used to determine the low frequency spectral level Ω_0 and angular corner frequency ω_c , which will be used in the determination of source parameters.

Results of the analysis provide a stable solution for the accelerometer recordings at an hypocenter distance of 4-10 km. The seismic moment is $M_0 = 3.5 \pm 0.9 \text{ E}+14 \text{ Nm}$ and the corresponding moment magnitude $M_w = 3.6 \pm 0.1$.

There is a difference of 0.2 magnitude units between the mean values of M_L and M_w and although the error bars increase if restrictions on epicenter distances are relaxed, this difference is currently being investigated in detail. Both magnitude calculations are based on displacement data. For M_L an additional Wood- Anderson filter is applied, that includes a 0.8 Hz high pass filter. For the larger events this filter's corner frequency approaches the corner frequency of the events and its influence is part of ongoing research. The outcome may have implications for the procedure used to determine M_L , but its effect is expected to be small (0.1-0.2 magnitude units).

In summary, we consider the $M_w = 3.6 \pm 0.1$ as the best magnitude estimate for the Huizinge earthquake. We will investigate closer the M_L - M_w relation to obtain a more robust and accurate rapid magnitude estimator for induced seismicity. However, we would like to note that earthquake magnitude estimates are inherently uncertain with 0.1 usually being the lowest possible uncertainty limit.

Comparison with other magnitude estimates

The magnitude reported by the EMSC, $M_L = 3.7$, is within the error bounds similar to the $M_w = 3.6$. The Geofon solution, $M_{LV} = 3.9$, local magnitude derived from the vertical component, is too high, but may be explained by using stations that are located in only a small azimuth range. Unfortunately, both EMSC and Geofon do not publish error bars on their magnitude determinations.

Source mechanism and parameters

Source mechanism

Based on polarity information from the first onsets of the seismic waves and amplitude ratio's between the P, SV and SH phases, no stable focal mechanism could yet be found. However, a previous event, $M_L = 2.7$, 600m south east of the current event happened on April 14, 2009. For this event a focal mechanism could be determined, being a normal fault with a strike of 320° , a dip of 66° and a strike of -105° [1].

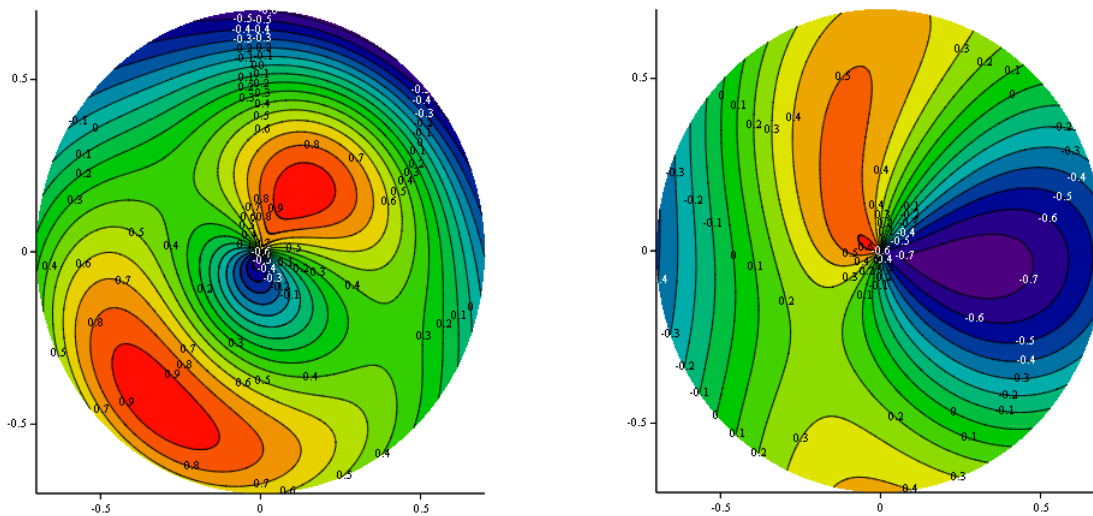


Figure 3, Source mechanism for the 2009, $M_L = 2.7$ Huizinge event. On the left the SV radiation pattern is shown, on the right SH radiation pattern. Radiation is shown in a lower hemisphere projection. Positive polarity is indicated in red, negative in blue.

Taking the 2009 event as an example, figure 3 shows the vertically (SV) and horizontally (SH) polarized shear wave radiation pattern. Due to a dipping fault surface and a small effect of the rake, the radiation pattern is complex.

Finding a stable solution for the source mechanism is important for understanding the earthquake process and will be used in geomechanical modeling. It also may explain the patterns we see in the intensity values.

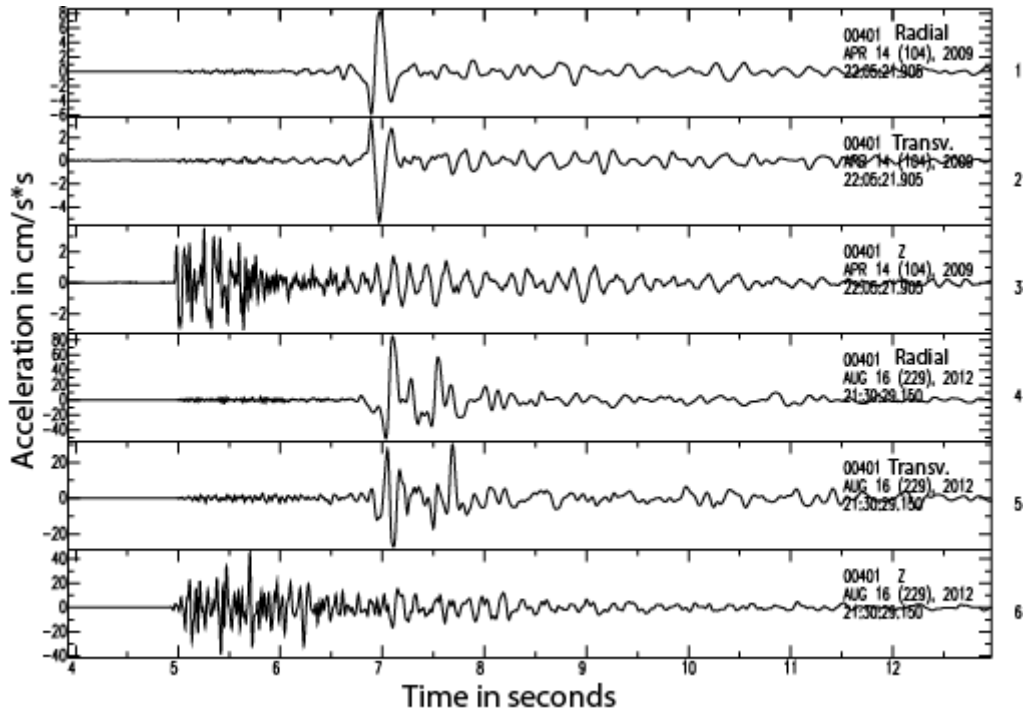


Figure 4. Comparison of acceleration recorded in station Middelstum-1 for the April 14, 2009, $M_L = 2.7$ (top three records) and the recent August 16, Huizinge event (bottom three records). From top to bottom: 090414- (1=radial, 2=transverse, 3=vertical) and 120816- (4= radial, 5=transverse, 6= vertical).

Comparison between the two closely spaced events near Huizinge is expected to provide more insight in the possible mechanism. However, being at similar epicenter distances of 2-3 km, the difference in azimuth is around 20 degrees and the polarity of the P waves is very different. Remarkable is the double S pulse for the recent Huizinge event and deserves extra attention, as it extends the duration of the strong shaking. Waveform inversion, using a detailed velocity model is expected to assist in constraining the mechanism. Both topics are subject of ongoing research.

Source parameters

Source parameters, such as the seismic moment, stress-drop, radius of a circular fault model and the average displacement on the fault have been estimated based on Brune's model [1].

	Corner frequency [Hz]	Stress-drop [bar]	Radius [m]	Average displacement [mm]
Accelerometers	1.9 ± 0.6	24 ± 18	460 ± 130	60 ± 38
Boreholes	2.4 ± 0.4	25 ± 16	340 ± 50	48 ± 19
All	2.2 ± 0.5	25 ± 9	390 ± 110	53 ± 28

Table 1. Source parameters for the Huizinge earthquake

As seen in Table 1, the accelerometers and borehole sensors give similar results. The event is characterized by a low corner frequency, around 2 Hz and a relatively high stress drop of 25 bars, compared to 17 bars for the $M_L = 3.5$, 2006 event near Westeremden [1]. Source radius is comparable between both events, while the average displacement of the Huizinge 2012 event is 60% larger, thus resulting in the large stress drop estimate.

Peak Ground Acceleration (PGA) and Peak Ground Velocity (PGV)

For the assessment of damage, an estimate of peak ground acceleration (PGA) or peak ground velocity (PGV) is required [1]. PGV values are derived from the PGA measurements by applying a recursive filter that includes removal of the instrument response and conversion to velocity.

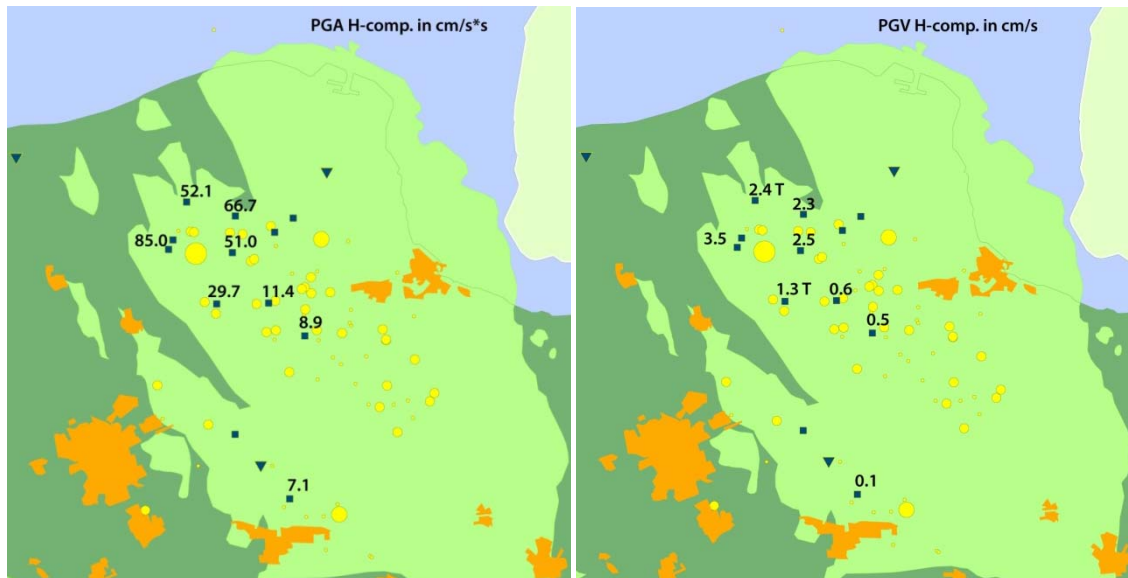


Figure 5. Maximum accelerations [a] and velocities [b] recorded by the KNMI accelerometer network. Indicated are maximum values, not average values. In b) PGV recorded in the transverse component is marked by "T".

The Huizinge event was recorded at 8 accelerometer stations at an epicenter distance between 2 and 18.5 km. The maximum horizontal peak ground acceleration (PGA) measured is 85 cm/s², corresponding to a peak ground velocity of 3.45 cm/s (Table 2). Figure 5a shows the variation of PGA over the region with a west-east trending maximum value close to the epicenter. This maximum corresponds to the radial component, while in north-south direction the maximum is found on the transverse component. This difference is due to the source mechanism.

station	PGA rad	PGA trans	PGA hor	PGA z	PGV rad	PGV trans	PGV hor	Epic. dist [km]
WSE	51.0	40.8	45.9	75	2.55	1.21	1.88	2.6
MID1	85.0	30.0	57.5	45.2	3.45	0.9	2.18	2.0
GARST	66.7	35.9	51.3	25.8	2.34	0.79	1.57	3.9
KANT	22.4	52.1	37.3	22.7	0.69	2.36	1.53	3.8
STDM	17.7	29.7	23.7	20.8	0.58	1.33	0.96	3.8
WIN	11.4	11.3	11.4	9.9	0.64	0.43	0.54	6.2
HKS	6.8	8.9	7.9	11.7	0.4	0.45	0.43	9.6
FRB2	4.0	7.1	5.6	5.1	0.1	0.11	0.11	18.5

Table 2. Measured values of PGA and PGV in 8 accelerometer stations from figure 5.

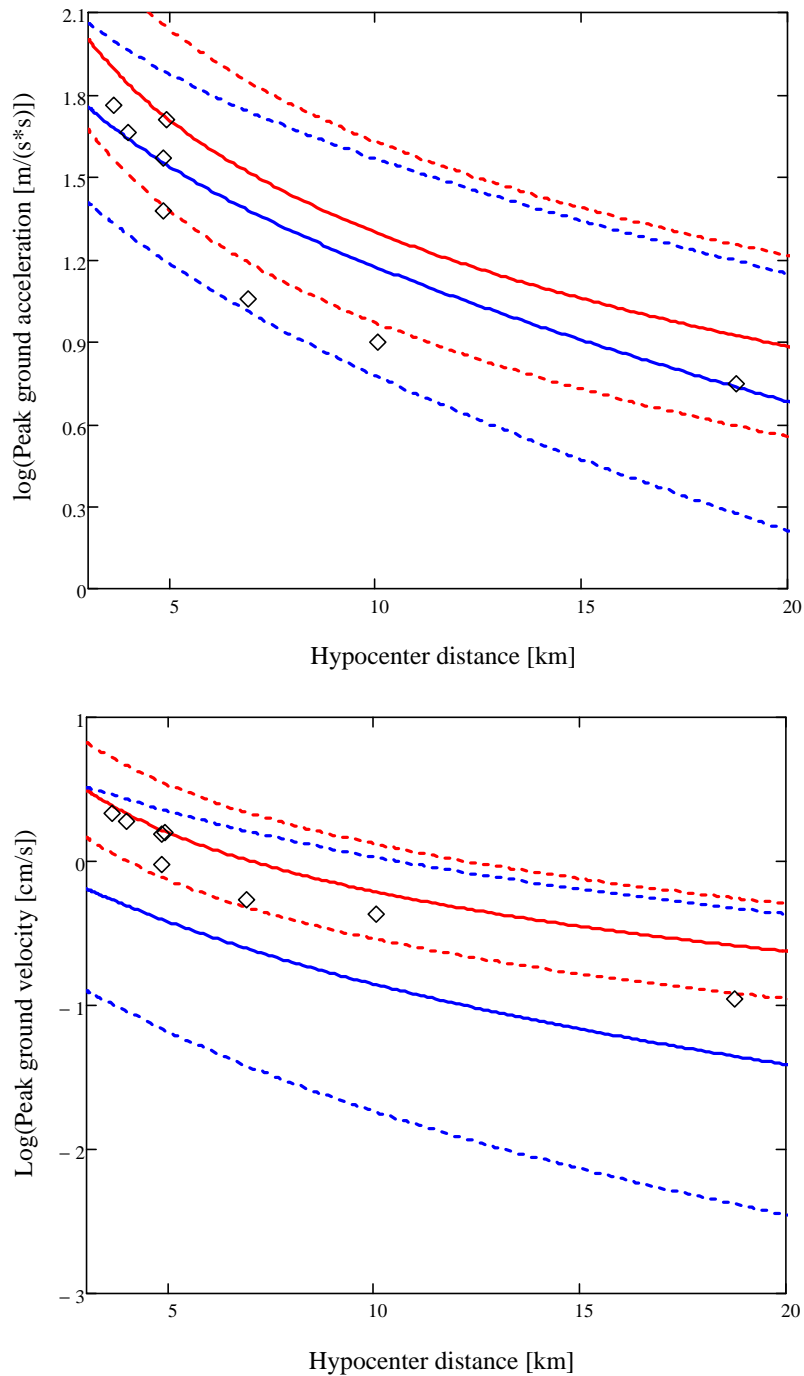


Figure 6. Measurements of PGA (top) and PGV (bottom) from the Huizinge event compared to models from [3, D04] in red and [4, D12] in blue. Uncertainties are indicated by dashed lines

These measurements provide a unique opportunity to test Ground Motion Prediction Equations (GMPEs) that were derived in the past. Two models were selected: D04, a model based on measured data from small shallow events recorded in the Netherlands [3] and D12, a more recent model based on a larger dataset of similar events [4].

For the PGA and PGV different definitions are used: 1] the maximum (peak) value on one of the horizontal components and 2] the geometric mean of the peaks of the two horizontal components. The latter is used in the GMPE's listed.

From the comparison of the data with predictions from the two models in figure 6, we conclude that for PGV model D04 fits the data within the error bars, while D12 underestimates the data. For the PGA measurements D12 is the better model, while D04 overestimates the data. The variance in the D12 model is large compared to D04, which might be caused by the different types of shallow seismicity from different regions used in the inversion.

Damage and PGV

Based on measured accelerograms near Roswinkel, an assessment was made of the damage probability for different building classes as a function of PGV [10]. This relation between damage probability and PGV was used in an assessment of the maximum damage due to a M=3.9 earthquake near the Bergermeer gasfield [11] and may also act as a guideline for damage assessment of the Huizinge event.

However, the signals recorded near Huizinge do show a different character, mainly due to the occurrence of two or three S-wave phases. Evaluation of response spectra, calculated from the accelerometer data, is required to further investigate the applicability of the aforementioned relation.

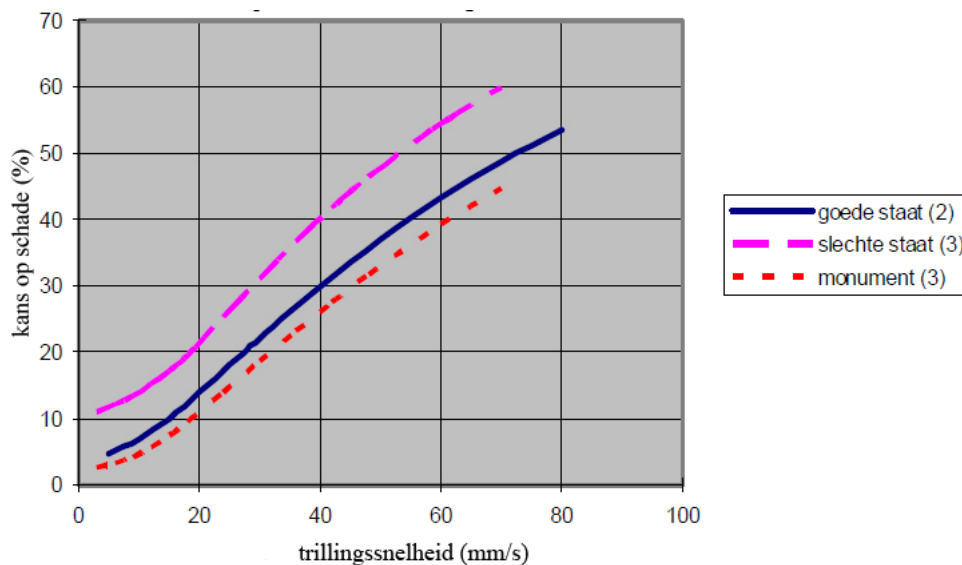


Figure 7. Damage probability (y-axis) versus PGV (x-value) for masonry buildings in a good state (blue), a bad state (purple) and monuments (red). Figure taken from [11].

The largest recorded PGV in the region is 34.5 mm/s, which is equivalent to a 20-35% probability of damage to masonry buildings. An evaluation of over 2000 damage reports in the region and comparison with the damage probability curves will be a good test-case for the applicability of the relation.

Source Duration

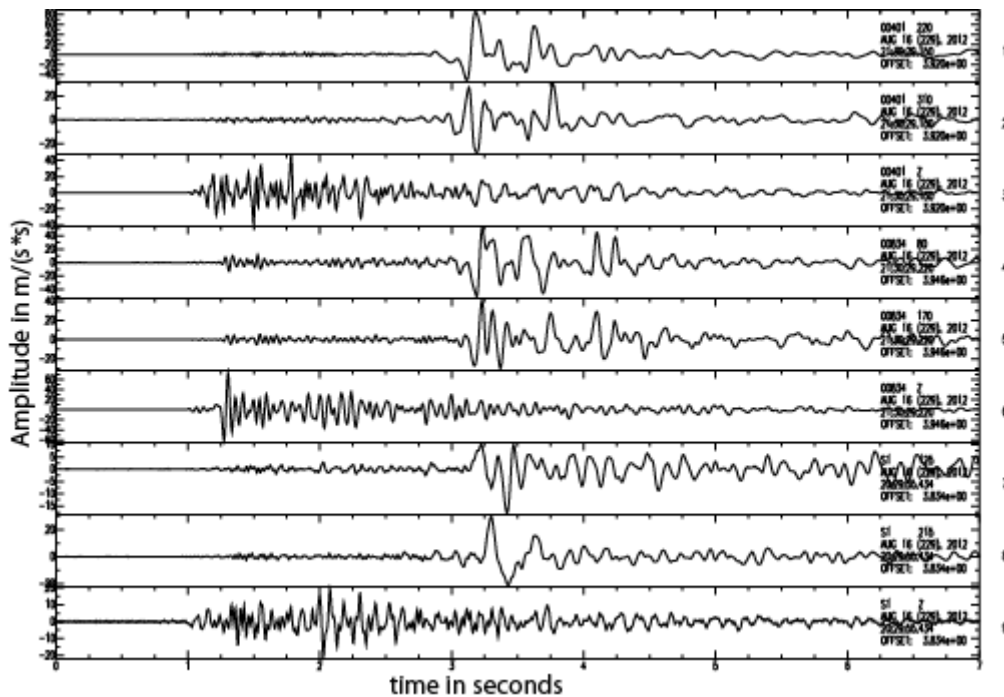


Figure 8. From top to bottom: accelerometer recording in station Middelstum-1 (1-3, radial, transverse and vertical)), Westeremden (4-6, rad, trans., vert.) and Stedum (7-9, rad, trans., vert.) for the August 16, 2012 Huizinge event.

The accelerometer data from the Huizinge event shows in some stations multiple S-phases, resulting in longer duration of the strongest motion from 0.2 to 1.5 seconds (Figure 8). The P wave recorded in Westeremden shows a complex onset and it is unclear if this is a source (rupture) effect or a local effect. Waveform modeling will be used to investigate the complexity of the waveforms, looking for an explanation of both phenomena. The salt layer on top of the reservoir, acting as a high velocity layer, varies strongly in thickness nearby the epicenter. Multiple reflections in the salt may be candidates to explain this pattern of multiple phases.

The effect of multiple S phases is not present in the 2009 event, as demonstrated in figure 4. In some other larger events in the region, a similar longer duration of the S-wave strong motion is reported in some of the stations, but certainly not all. Also these records will be used in the waveform modeling.

Intensity

The KNMI operates a Web site which provides an inquiry where people can contribute with their experiences during local earthquakes (<http://www.knmi.nl/seismologie/seismoenquete.html>). These inquiries form the basis of an evaluation of intensities. Intensity data, describing the felt effects from the Huizinge event, are compared to measured PGA and PGV values in the region.

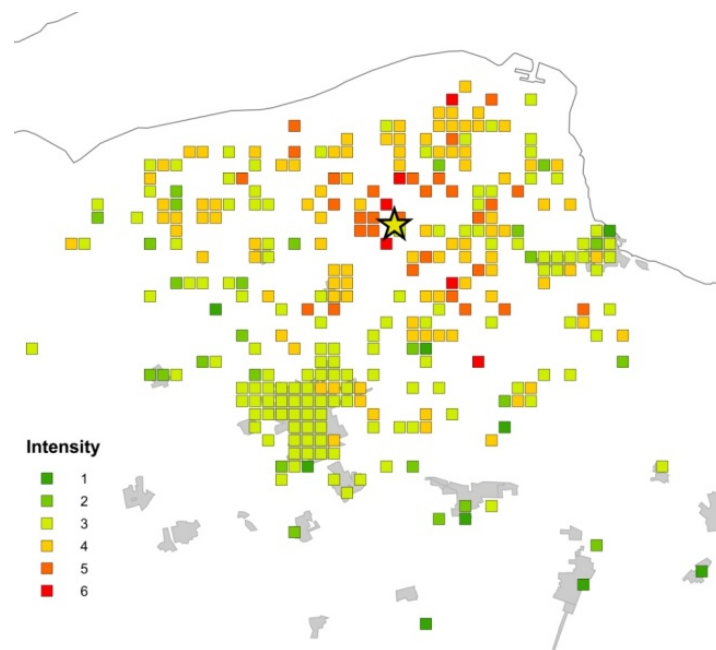


Figure 8. Community Internet intensities, for the 2012 Huizinge earthquake (epicenter marked by a star). Communities are based on the Dutch zip code system and averaged over 1 km² areas. Cities are shown in grey.

Incoming responses to the inquiries are processed using an approach developed at KNMI for induced earthquakes in the Netherlands, based on the Community Intensity Map approach [8]. Weights are assigned to the different categories in the inquiries and intensities calculated as a weighted sum. This method has been calibrated using a number of shallow induced events for which also a manual interpretation exists. Average values of Community Internet Intensities (CII) for the Huizinge event are shown in figure 8. Although many small communities exist in the region, people living in the larger cities, like Groningen south-east of the epicenter or Delfzijl to the east, dominate the response.

Figure 9 shows the isoseisms, obtained from the Community Internet Intensities in figure 8. Isoseisms are calculated using a kriging technique. In order to diminish the effect of spatial undersampling, a background intensity net was introduced. All processing was carried out using ArcMap software and the isoseisms are calibrated using comparison with manually interpreted isoseisms for past events.

The isoseisms fit well with a shallow source at 3 km depth. The Macroseismic epicenter, taken as the center of the intensity VI contour, is located north-east of the instrumental epicenter. This difference may be explained by the source mechanism. However, details in the intensity contours are also

influenced by the population density, e.g. to the south-west the effect of the city of Groningen is clearly visible and therefore one should be cautious with the interpretation of the contours. Intensity VI is measured in a limited region at < 4km from the macroseismic epicenter.

EMS 98	Short description	Additional info
1	Not felt	Not felt by anyone
2	Scarcely felt	Vibration is felt only by individual people at rest in houses, especially on upper floors of buildings.
3	Weak	Felt indoors by few, people at rest feel swaying or light trembling, noticeable shaking of objects
4	Largely observed	The earthquake is felt indoors by many people, outdoors by few. A few people are awakened. The level of vibration is possibly frightening. Windows, doors and dishes rattle. Hanging objects swing. No damage to buildings
5	Strong	The earthquake is felt indoors by most, outdoors by many. Many sleeping people awake. A few run outdoors. Entire sections of all buildings tremble. Most objects swing considerably. China and glasses clatter together. The vibration is strong. Topheavy objects topple over. Doors and windows swing open or shut.
6	Slightly damaging	Felt by everyone indoors and by many to most outdoors. Many people in buildings are frightened and run outdoors. Objects on walls fall. Slight damage to buildings; for example, fine cracks in plaster and small pieces of plaster fall
7	Damaging	Most people are frightened and run outdoors. Furniture is shifted and many objects fall from shelves. Many buildings suffer slight to moderate damage. Cracks in walls; partial collapse of chimneys.

Table 3. Overview of the descriptions belonging to the EMS98 intensity grades.

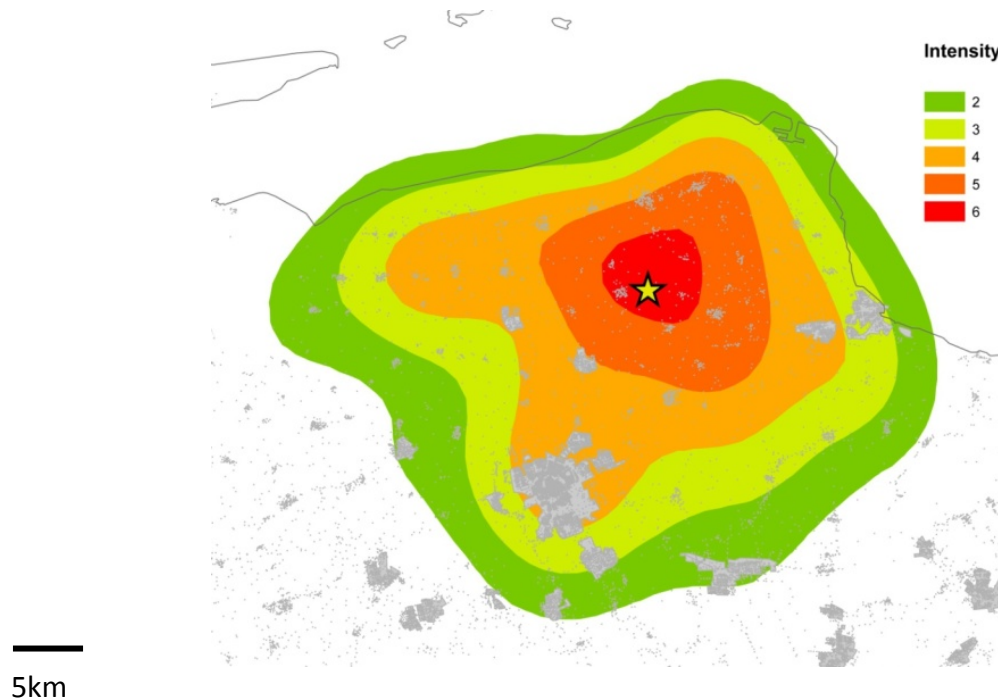


Figure 9. Isoseisms for the 2012 Huizinge event.

Implications for hazard analysis

The last update of the hazard analysis for the region [1] included all data until 2010. The Huizinge event allows us to extend the dataset to September 2012 and investigate the hazard for the Groningen field in more detail, since the dataset for this field now contains 190 events of $ML \geq 1.5$. A new public dataset on average annual production became recently available (www.nlog.nl/en/oilGas/oilGas.html) and could be used to compare annual production to seismicity.

Cumulative energy

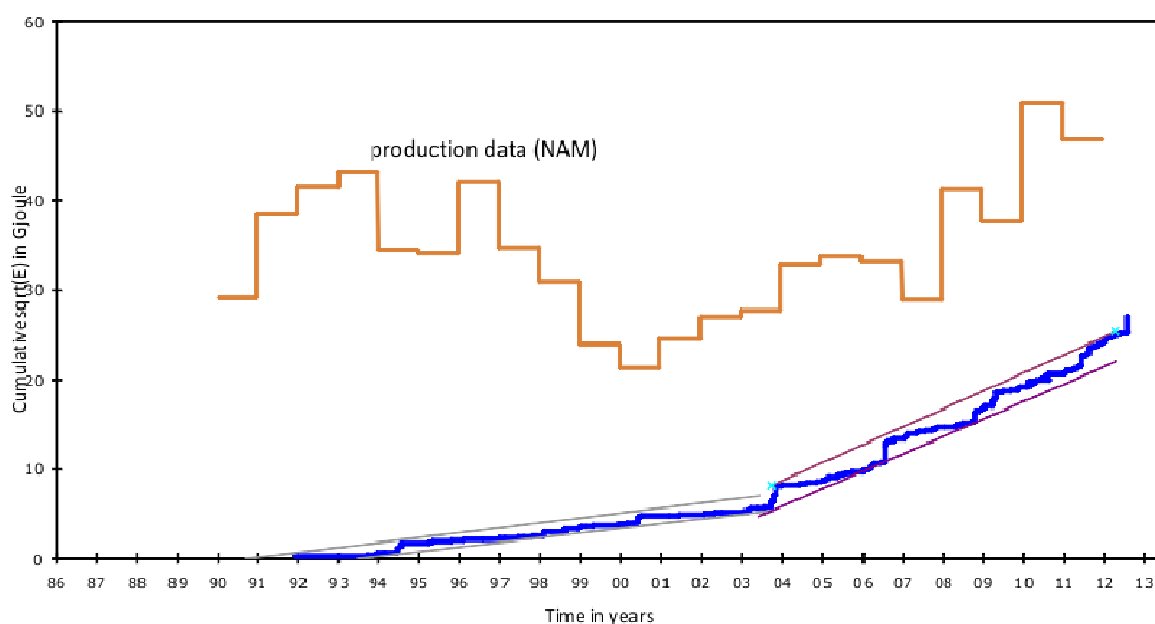


Figure 10: Cumulative square root of the energy released in the events in the Groningen field (blue) in Gjoule compared to average annual gas production in Billion Cubic Meter (BCM). Also shown are the linear models describing the cumulative seismic energy release.

We estimated the cumulative seismic energy release with time for the period 1986-2012, following the procedures explained in [1]. The increase in the rate of seismic energy, which was reported in [1], based on data for all gas fields for the period 1986-2010 continues. Selecting only the Groningen field data from the database the increase in the rate of seismic energy becomes even more pronounced (Figure 10).

The break in the energy curve correlates with the production data. The driving force behind the seismicity is thought to be differential compaction [9]. Increased production since 2001 may therefore explain the increased rate of seismic energy release starting around 2003. The high production in the period 1990-1997 may have resulted in relative low levels of seismicity because not enough compaction was available at that time.

As discussed in [1], the increased rate of seismicity implies a breakdown of the stationarity assumption in the seismic hazard assessment.

Frequency-magnitude relation

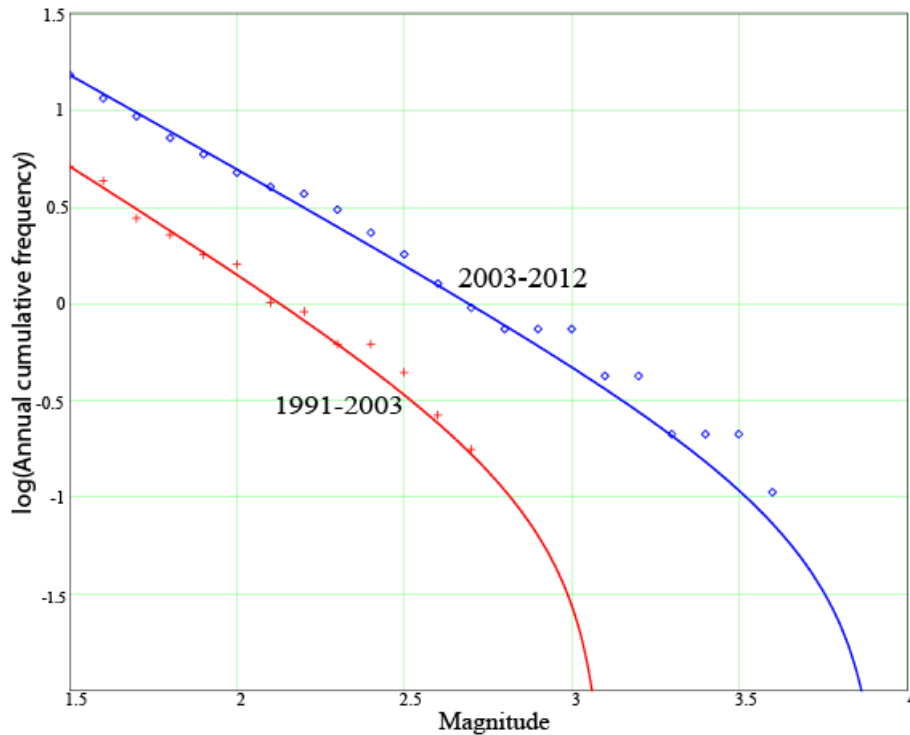


Figure 11. Annual cumulative frequency for two time periods (1991-2003 and 2003-2012). Seismicity rate (GR a - values) differs, but the b -values are equal within their error bounds.

Following the methods described in [1], we calculated the frequency magnitude relation (FMR) for the Groningen field only. Since the assumption of stationarity over the total period where seismicity is observed in the Groningen field seems to be not valid any more, the data set is split-up in two periods: 1991-2003 and 2003-2012. Figure 11 shows the FMR for the two time periods.

The FMR curves consists of a Gutenberg-Richter (GR) part, described by a linear relation, and a non-linear part for the higher magnitudes. Parameters a , the seismicity rate, and b , the slope of the GR relation are calculated using a maximum likelihood methods (see [1] for references).

For Groningen (1991-2003) the best result, using the method of Page is $b = 1.08 \pm 0.25$, $a = 2.33 \pm 0.37$ and $M_{\max} = 3.1$. This method is dependent on an assumption for M_{\max} , but this has not a large influence (e.g. with $M_{\max} = 3.3$: $b = 1.14 \pm 0.29$). Processing the data for Groningen for the period 1996-2003, where the magnitude of completeness is 1.5, leaving-out the observation of detected events in the period 1991-1996, gives as best estimate with $M_{\max} = 3.1$: $b = 1.41 \pm 0.41$ and $a = 2.84 \pm 0.61$. For this reduced dataset, the error in the b -values significantly increased and this demonstrates the importance of carefully constraining a sparse dataset.

For the period 2003-2012 the curve is less well behaved, but contains 3 times more data and gives a best fit, using the same method, of $b=1.09 \pm 0.17$, $a=2.82 \pm 0.25$ at $M_{\max}=3.9$. The fit is best for the lower magnitude range and worse for the higher magnitudes. Using higher values for M_{\max} only results in a higher b -value, while a lower b -value would give a much better fit.

We conclude from the analysis that both GR curves are characterized by a similar value of b , but at a different seismicity rate a . Since the b -value gives an indication of the mechanism behind the seismicity the fact that the change in behavior of the system is only due to the seismicity rate is reassuring.

Maximum magnitude

Groningen field

Since there is only information available on the statistics of seismicity for this region, no estimate of the maximum probable magnitude for the Groningen field could be made on the basis of estimated available fault surface or the reactivation potential of faults and the average slip from geomechanical modeling.

Therefore, a Monte Carlo simulation [1] has been applied to the seismicity data from the Groningen field. In this simulation artificial datasets are generated by randomly varying the calculated annual cumulative frequencies within their error bounds and fit each dataset to a bounded frequency-magnitude relation. Result is a Poisson distribution of values for M_{\max} . In this procedure, values for $M_{\max} > 5.5$ are discarded, being regarded unrealistic and an artifact of the method. Results for the Groningen field data show a flat probability density function, which could not be interpreted in terms of a Poisson distribution. Therefore, it was concluded that no reliable estimate can be given for the M_{\max} of the Groningen field alone.

Until now, the assumption was that if we take the statistics of all fields, this would give a good indication of a M_{\max} for individual fields. This was a necessary step, since the dataset for individual fields was too small to draw conclusions. Only recently, this changed for the Groningen field.

Other hydrocarbon fields in the Netherlands

The Groningen dataset dominates the induced seismicity database for the Netherlands since 2003, therefore also the M_{\max} estimates from statistics for other fields may be questioned. In some instances, e.g. the Bergermeer field, independent information on available fault surface and estimates of average slip from geomechanical modeling are available[12][13]. These estimates confirm the $M_{\max}=3.9$ estimate from statistics. Since most of the smaller fields do contain faults of limited size, we do not see a reason to change the existing M_{\max} for the other fields.

Hydrocarbon fields outside the Netherlands

An alternative approach to estimate the maximum possible magnitude is to look for analogues in other areas with (similar types of) induced seismicity. Here we have to take care to make a distinction between triggered and induced seismicity. In triggered seismicity the stress perturbations that are released during an earthquake are primarily due to natural tectonic processes; the human activities merely trigger the earthquakes, perhaps sometime ahead of their natural occurrence. In induced seismicity the stress perturbations that are released during an earthquake are primarily induced by the human activities themselves, as is the case in Groningen. The field is located in an area that we regard as aseismic from a natural perspective. We therefore do not expect any triggered seismicity.

Perhaps the closest analogue is found in the gas fields of Northern Germany. These fields are located in the same sedimentary sequence as the Groningen field, in a similar tectonic setting, albeit a bit deeper (4.5-5.0km). The Rotenburg event of October 20, 2004 took place in the direct vicinity of a gas field in production and had a moment magnitude of $M_w = 4.4$ ($M_L = 4.5$). It is probably also an induced event [15]. Due to the limited number of events in Northern Germany a statistical analysis is not possible.

The Ekofisk oilfield in the North Sea is located at a similar depth as the Groningen field in the sedimentary basin of the Dutch Central Graben. The largest earthquake in the surroundings of the Ekofisk field was the May 7, 2001 event with moment magnitude M_w 4.1-4.4 [16]. Although the area is not completely void of natural seismicity this largest event was most probably induced, although its nature was quite different from the events in Groningen. The Ekofisk event took place in the overburden on a very large sub-horizontal plane with small displacement. The subsidence induced by the oil recovery is in the order of meters and the event followed an unintended water injection.

The Lacq gas field in the South of France has a history of more than 1000 micro-earthquakes with local magnitudes up to M_L 4.2 [17,18,19]. The depth is similar to Groningen, but sedimentary and tectonic context is quite different, with a less compacting chalk reservoir and the vicinity of the Pyrenees.

An event of short-period-body-wave magnitude $m_b L_g$ 4.3, on April 9, 1993, was probably induced by the gas extraction from the Fashing field in South-Central Texas [20]. The field is located in a limestone reservoir under an anticlinal structure at depth similar to the Groningen field. In the same area on October 20, 2011 an event took place with magnitude 4.8, as reported in the public media. For this event we have not found a scientific publication.

Higher magnitude events have also been observed in the neighborhood of hydrocarbon reservoirs (e.g., Gazli 1984, M_L 7.2; Coalinga 1983, M_L 6.7), however these have been identified as natural or triggered rather than induced. In recent years overviews of induced seismicity in hydrocarbon fields are published [21,22] and for human induced events [23]. The latter includes both triggered and induced earthquakes. In [21] the author remarks "Induced seismicity in hydrocarbon fields is typically small to moderate ($M_L \leq 4.5$)".

To conclude, the magnitudes of the largest induced events in hydrocarbon reservoirs, as reported in the scientific literature, remain, if rounded upwards, below $M_L = 5.0$. One has to keep in mind, however, that the comparison is made for hydrocarbon fields in different geological settings and tectonic regions. Also, enough existing fault surface should be available to accommodate the movement of a larger event.

Consequences for Groningen

Based on statistics only, no reliable estimate could be obtained of a maximum probable earthquake for the Groningen field. Further research using additional information from geology and geomechanical modeling is expected to provide additional constraints on the possible value of the M_{max} . Until this information is available, we estimate a conservative upper limit for M_{max} at magnitude 5.0.

An estimate of the intensity that corresponds to a $M_{max} = 5.0$ is difficult to assess. Magnitude-intensity relations have a large standard deviation. A rough estimate will be that intensities will reach an intensity VII (Table 3).

Conclusions

The earthquake on August 16, 2012, near Huizinge (Groningen) is the largest induced earthquake ever recorded in the Netherlands related to hydrocarbon production. A detailed analysis shows

1. The Huizinge event is located in the area of highest activity in the Groningen field within the community of Loppersum.
2. The moment magnitude of the event is $M_w=3.6 \pm 0.1$, which is larger than the original estimate of the local magnitude $M_L = 3.4 \pm 0.1$. The M_L - M_w relation is subject of ongoing research.
3. The source is characterized by a radius of 390 ± 110 m, an average displacement of 5 ± 3 cm and a stress-drop of 25 ± 9 bar. Polarity inversion did not provide a stable mechanism yet, waveform modeling is expected to provide results.
4. Accelerometer recordings at epicenter distances of 2-10 km show values of PGA up to 85 cm/s^2 and PGV up to 3.45 cm/s. At these values a damage probability of 20-35% exists for masonry structures, although this relation is valid only for events of short duration. It is shown that Ground Motion Prediction Equations derived for small shallow earthquakes predict the measurements.
5. Multiple S-wave phases have been recorded, extending the duration of the strong motion. This longer duration was also observed by local people.
6. Maximum intensity VI is observed in a limited region (<4 km) around the macroseismic epicenter.
7. For the Groningen field an update of the hazard analysis is carried out, including an estimate of the maximum probable magnitude. Based on cumulative energy calculations the dataset was divided into two segments (1991-2003) and (2003-2012). Both segments are characterized by a constant b-value, but different seismicity rate. Comparison with average annual production data shows a correlation between seismicity rate and production.
8. A value for M_{max} could not be derived for the Groningen field, due to the nature of the frequency-magnitude relation.
9. A literature study of induced seismicity in other hydrocarbon fields indicate maximum recorded events between $M_L = 4.2$ (Lacq) and $M = 4.8$ (Fashing). Following only these observations we do not expect larger events to occur in the Groningen field, i.e. a maximum probable magnitude below $M_L = 5.0$.

References

- [1] Dost, B., F. Goutbeek, T. van Eck and D. Kraaijpoel, 2012, Monitoring induced seismicity in the North of the Netherlands: status report 2010, *KNMI Scientific report*; WR 2012-03.
- [2] Kraaijpoel, D. and B. Dost, 2012, Implications of salt-related propagation and mode conversion effects on the analysis of induced seismicity, *Journal of Seismology*, DOI 10.1007/s10950-012-9309-4
- [3] Dost, B., T. Van Eck and H. Haak, 2004, Scaling of peak ground acceleration and peak ground velocity recorded in the Netherlands, *Bollettino di Geofisica Teorica ed Applicata*, 45,3: 153-168.
- [4] Douglas, J., B. Edwards, V. Convertito, N/ Sharma, A. Tramelli, D. Kraaijpoel, B.M. Cabrera, N. Maercklin and G. De Natale, 2013, Predicting ground motion from induced earthquakes in geothermal areas, *submitted to Bul. Seism. Soc. Am.*, 2012.
- [5] Hanks, T.C. and H. Kanamori, 1979, A Moment Magnitude Scale, *Journal of Geophys. Research*, 84: 2348-2350.
- [6] Aki, K. and P.G. Richards, 1980, *Quantitative Seismology, theory and methods*, W.H. Freeman and company, San Francisco, 932 pp.
- [7] Anderson, J.G. and S. Hough, 1984, A model for the shape of the Fourier amplitude spectrum of acceleration at high frequencies, *Bulletin of the Seismological Society of America*, 74: 1969-1994.
- [8] Wald, D.J., V. Quitoriano, L.A. Dengler, and J.W. Dewey, 1999, Utilization of the Internet for Rapid Community Intensity Maps, *Seismological Research Letters*, 70: 680-697.
- [9] Dost, B. and H.W. Haak, 2007, Natural and induced seismicity, in Th. E. Wong, D.A.J. Batjes, and J. de Jager. Eds., *Geology of the Netherlands*, Royal Netherlands Academy of arts and Sciences, 223-229.
- [10] Van staalduinen, P.C. en C.P.W. Geurts, 1998, De relatie tussen schade aan gebouwen en lichte, ondiepe aardbevingen in Nederland: inventarisatie, TNO rapport 97-CON-R1523-1, 98pp.
- [11] Van Kanten-Roos, W., B. Dost, A.C.W.M. Vrouwenfelder and T. van Eck, 2011, Maximale schade door geïnduceerde aardbevingen: inventarisatie van studies met toepassingen op Bergermeer. TNO-KNMI report (also published as appendix in [1]).
- [12] Logan, J.M., N.G. Higgs, J.W. Rudnicki, 1997, Seismicity risk assessment of a possible gas storage project in the Bergermeer field, Bergen concession, *Report to BP*, 137pp.
- [13] Muntendam-Bos, A.G., B.B.T. Wassing, C.R. Geel, M. Louh and K van Thienen-Visser, 2008, Bergermeer Seismicity Study, *TNO report 2008-U-R1071/B*, 95pp.

- [14] Castagna, J.P., Batzle, M.L. and Eastwood, R.L., 1985, Relationships between compressional wave and shear-wave velocities in clastic silicate rocks: *Geophysics*, 50, 571-581.
- [15] Dahm, T., F. Krueger, K. Stammler, K. Klinge, R. Kind, K. Wylegalla and JR Grasso, 2007, The 2004 M_w 4.4 Rotenburg, Northern Germany, Earthquake and Its Possible Relationship with Gas Recovery , *Bull. Seism. Soc. Am.*, 97: 691-704, DOI: 10.1785/0120050149.
- [16] Ottemoeller, L., H.H. Nielsen, K. Atakan, J. Braunmiller, and J. Havskov, 2005, The 7 May 2001 induced seismic event in the Ekofisk oil field, North Sea, *J. Geoph. Res.*, 110, B10301, doi: 10.1029/2004JB003374.
- [17] Maury, V., J.R.Grasso and G. Wittlinger, 1990, Lacq Gas Field (France): Monitoring of induced Subsidence and Seismicity Consequences on Gas Production and Field Operation., *Society of Petroleum Engineers (SPE)*, SPE 20887.
- [18] Feignier, B. and J.R. Grasso, 1990, Seismicity Induced by Gas Production: I. Correlation of Focal Mechanisms and Dome Structure, *Pure and Applied Geophysics*, 134: 405-426.
- [19] Grasso, JR., 1992, Mechanics of seismic instabilities induced by the recovery of hydrocarbons, *Pure appl. Geophysics*, 139:507-534.
- [20] Davis, S.D., P. A. Nyffenegger and C. Frohlich, 1995, The 9 April 1993 Earthquake in South-Central Texas: Was It Induced by Fluid Withdrawal? *Bull. Seism. Soc. Am.*, 85: 1888-1895.
- [21] Suckale, J., 2009, Induced seismicity in hydrocarbon fields, *Advances in geophysics*, 51: 55-106
- [22] Suckale, J., 2010, Moderate-to-large seismicity induced by hydrocarbon production, *The Leading Edge*, 29: 310-319
- [23] Klose, C. D., 2013, Mechanical and statistical evidence of the causality of human-made mass shifts on the Earth's upper crust and the occurrence of earthquakes, *Journal of Seismology*, 17:109-135 DOI 10.1007/s10950-012-0321-8.